Strength Demand Spectra with Uniform Damage Level in Lifetime of Structure

Y. Sunasaka*, A. S. Kiremidjian**, K. Toki***

* Dr. of Eng., Kajima Corporation, 6-5-30, Akasaka, Minato-ku, Tokyo 107-8502
** Dr. of Eng., Professor, Dept. of Civil and Environmental Eng., Stanford Univ., Stanford, CA94305-4020
***Dr. of Eng., Professor, Graduate School of Eng., Kyoto Univ., Yoshida Honmachi, Sakyo-ku, Kyoto 606-8501

Damage to modern engineering structures was caused by recent great earthquakes and their aftershocks. In this paper, damage spectrum is used to evaluate the damage potential of large earthquakes and aftershocks. The damage index proposed by Park and Ang and a bilinear model are used to calculate the damage spectrum. Ground motions during recent great earthquakes and their aftershocks are studied to evaluate their damage potential. Then, a method is proposed for evaluating the strength demand spectra with uniform damage level in the lifetime of a structure considering mainshock-aftershock earthquake.

Key Words: Damage potential, mainshock-aftershock sequences, damage spectrum, strength demand spectrum, ground motion

1. Introduction

Large earthquakes and the aftershocks that follow them have caused extensive structural damage resulting in significant losses of lives and property. For example, it was reported that an aftershock of the 1987 Whittier Narrows earthquake increased the damage of the I-5/I-605 separator that had been caused by the mainshock[1]. The 1990 Philippine earthquake that consisted of two distinct earthquakes separated by about a minute's interval caused severe structural damage[2]. An aftershock of the 1999 Kocaeli earthquake caused extensive damage to structures around Duzce in Turkey. Similarly, aftershocks of the 1999 Chi-Chi earthquake caused extensive damage to structures in Taiwan.

Aftershocks of major earthquakes may be as large as ordinary locally damaging shocks. Moreover, the epicenters are likely to be distributed over a wide area; a large aftershock may originate closer to a center of population, and cause more damage there, than the main earthquake.

In order to consider aftershock effect on structural safety, the damage potential of ground motions during recent great earthquakes and aftershocks should be studied and their characteristics should be identified, first. Then, the damage potential of ground motions should be evaluated for the sequence of main earthquake and aftershocks. Such an approach is presented in this paper. Then, a method for evaluating the strength demand spectra with uniform damage level in the lifetime of a structure considering mainshock-aftershock earthquake sequences is proposed.

2. Damage spectrum

In this paper, the damage spectrum of ground motion during an earthquake is used to estimate its damage potential[3),4)]. The damage spectrum is defined as a damage index of single -degree-of-freedom (SDOF) system with natural period ranging from 0.05 to 5.0 sec. The damage index proposed by Park and Ang[5] is an appropriate tool to evaluate the damage to concrete structure during earthquakes. The method, however, is not contingent upon the use of this damage index and other damage indices can be used.

This index is expressed as a linear combination of the maximum normalized deformation and the hysteretic energy dissipation as follows:

$$D = \frac{\delta_m}{\delta_u} + \beta \int \frac{dE}{(Q_y \delta_u)} \quad \cdots\cdots\cdots\cdots (1)$$

where D is the damage index, an empirical measure of damage, δ_m is the maximum response deformation, δ_u is the ultimate deformation capacity under static loading, Q_y is the calculated yield strength, dE is the incremental dissipated hysteretic energy, and β is the coefficient for cyclic loading effect. $D \geqq 1$ indicates total damage or collapse. $0<D<0.7$ shows the slight damage, and $0.7<D<1.0$ shows severe damage. The limiting value of D

(i.e., damage capacity of a member) is lognormally distributed with a mean of 1.0 and a standard deviation of 0.54.

D(T, ξ) is defined to be damage spectra for SDOF system with a bi-linear force-deformation characteristics subjected to a specified ground motion. For a given structural period T and damping ξ, D(T, ξ) is equal to the Park and Ang's damage index. The parameters of the SDOF system and the damage index are shown in Table 1. The yield strength is set to be 40% of the weight of the SDOF (that is, the yield strength ratio to be 0.4, hypothetical value corresponding to the seismic coefficient of 0.2). The ultimate deformation capacity is set to be four times of the yield deformation. Park and Ang et al.[9] studied the value of the parameter β in equation (1). Based on their study, it is appropriate to assume that the value of the parameter β is 0.05, when the force-displacement relationship is bi-linear. These values are used just for a relative estimation of damage potential of ground motions.

Table 1 Basic parameters for analysis

SDOF Model	damping ratio ξ	0.05
	second stiffness k_2	$0.05k_1$
	yield strength Qy	0.4W
Damage Index	coefficient β	0.05
	ultimate deformation capacity δu	$4\delta y$

k_1: initial stiffness, W: weight of the SDOF, δy: yield deformation

3. Damage potential of aftershock ground motions

In order to study the damage potential of ground motions during aftershocks, relatively large ground motion record sets from both the mainshock and the aftershocks are needed. However, such record sets are very few. Several of these are discussed in this section.

The mainshock of the Coalinga, California earthquake occurred on May 2, 1983 with magnitude 6.5. Then an aftershock with magnitude 6 occurred on July 22, 1983. At several stations, relatively large ground motions were recorded during the aftershock. The observed ground motion during the mainshock and aftershock are shown in Figure 1. The damage spectra of the ground motions during the mainshock and aftershock are also shown in Figure 1. The damage spectra of ground motions in a sequence of mainshock-aftershock are calculated considering cumulative damage related with both the response deformation and the dissipated hysteretic energy of the SDOF during the sequence. In this example, the damage indices due to the mainshock and the aftershock are larger than those due to the mainshock alone in the natural period range smaller than 0.4 sec.

The mainshock of the Whittier Narrows, California earthquake occurred on October 1, 1987. Then an aftershock occurred on October 4, 1987. Relatively large ground motions were recorded during the aftershock. The damage spectra of the observed ground motions during the mainshock and aftershock are shown in Figure 2. In this example, it is found that the damage indices due to the mainshock and the aftershock combined are larger than those due to the mainshock alone in the natural period range between approximately 0.2 and 0.4 sec.

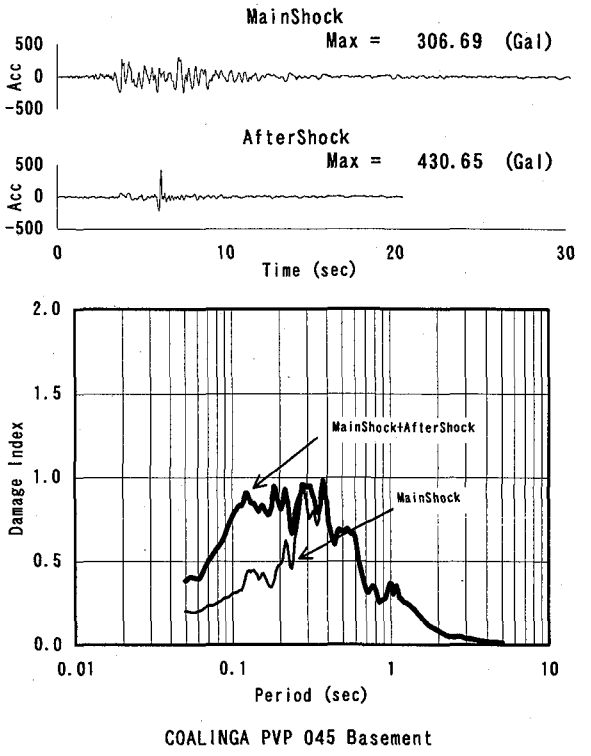

Figure 1 Recorded ground motions during the 1983 Coalinga earthquake and damage spectra

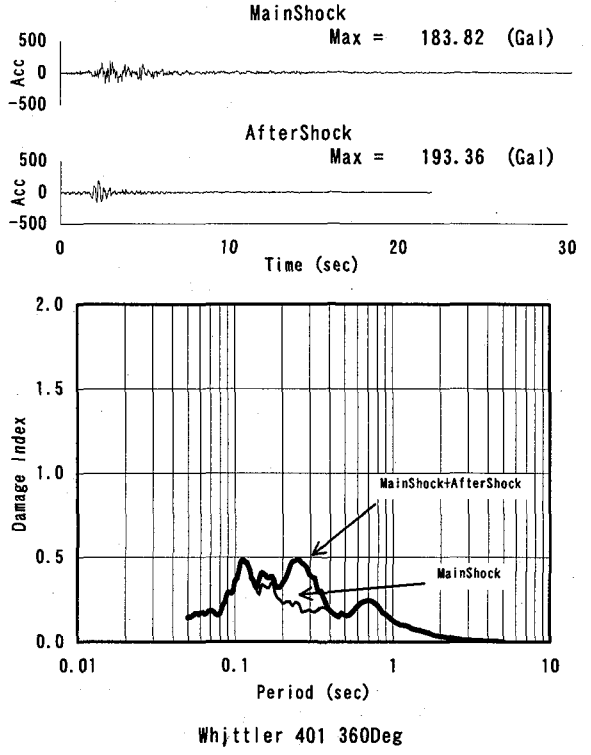

Figure 2 Recorded ground motions during the 1987 Wittier Narrows earthquake and damage spectra

Based on the examples presented herein, it can be concluded that the combination of mainshock-aftershock ground motions can be considerably more damaging to structures than the ground motions from the mainshock alone. What is interesting to observe is that structures that may have experienced relatively little damage from the mainshock have greater damage index following the aftershock. For example, the damage index from the mainshock at the natural period of 0.25 sec. in the Whittier Narrows earthquake is about 0.2, but it increases to a maximum of 0.5 following the aftershock.

4. Evaluation of strength demand spectra with uniform damage level in lifetime of structure

Earthquake events are typically composed of foreshock, mainshock and aftershock sequences. The mainshock in most cases releases the largest amount of energy and thus causes the most damage and destruction. Aftershocks, however, have also been known to cause considerable damage and are particularly detrimental to structures that have been weakened by the mainshock. In this section, a probabilistic occurrence model of mainshock-aftershock sequences[7], and a simulation methodology for evaluation of the damage potential of ground motions considering mainshock-aftershock earthquake sequences in the desired design period of a structure are presented. Then, a method for evaluating the strength demand spectra with uniform damage level in the lifetime of a structure considering mainshock-aftershock earthquake sequences is proposed.

4.1 Modeling of mainshock-aftershock sequences

4.1.1 Mainshocks

Earthquake occurrences are inherently rare and random in nature. Thus, they are frequently represented using stochastic models. The most commonly used model for earthquake occurrence is the Poisson model. In this model, the interarrival times are independent and exponentially distributed as follows:

$$f_T(t) = \lambda \exp(-\lambda t) \quad \cdots\cdots\cdots\cdots\cdots\cdots (2)$$

where $f_T(t)$ is the probability density function of interarrival time t, and λ is the average occurrence rate. Other models for mainshock occurrences include the time and slip predictable models of Anagnos and Kiremidjian[8] and Kiremidjian and Anagnos[9]. Application of these models depends largely on the availability of data for the region to be studied.

For simplicity, the rate of earthquake occurrences of mainshocks is considered to follow the Gutenberg and Richter relationship given as follows:

$$N(M) = \alpha \exp(-\beta M) \cdots\cdots\cdots\cdots\cdots\cdots (3)$$

where N(M) is the number of earthquakes with magnitude greater than or equal to M, and α, β are the zone-dependent constants. The probability density function of magnitudes of mainshocks is derived from equation (3):

$$f_M(m) = \frac{\beta e^{-\beta m}}{e^{-\beta M_{min}} - e^{-\beta M_{max}}} \quad \cdots\cdots\cdots (4)$$

where M_{min} is the minimum magnitude to be considered in the analysis, and M_{max} is the maximum magnitude at the site.

The choice of magnitude distribution depends on whether or not the magnitude is to be bounded between the minimum and maximum value. Thus, if the magnitude is limited, then equation (4) is the appropriate probability distribution. In the development of the mainshock-aftershock occurrence model, the minimum and maximum magnitudes need to be considered. Therefore, equation (4) will be used to describe the magnitudes of mainshocks. Other models for earthquake magnitudes have been proposed but will not be considered in this paper.

4.1.2 Aftershocks

The number and magnitude of aftershocks following a mainshock have been shown to decay in time. The duration over which large aftershocks occur is relatively short in comparison with the interarrival time of the mainshock, and has no significant effect on the occurrence of the mainshock. Thus, only a magnitude distribution model of aftershocks is needed.

It is assumed that the Gutenberg and Richter formula (3) applies to the distribution of magnitudes of aftershocks[10]. For an aftershock magnitude of M=c, the number of aftershocks can be estimated from the following relationship:

$$N_a(c) = \alpha \exp(-\beta c) \cdots\cdots\cdots\cdots\cdots\cdots (5)$$

where $N_a(c)$ is the total number of aftershocks with magnitudes greater than or equal to c, α and β are constants.

Characteristics of aftershocks appear to depend on their mainshocks. In particular, the number of aftershocks and the β -value depend on the magnitude of the mainshock. Thus, the following relationships can be obtained from earthquake data.

$$\ln[N_a(c)] = a + b M_0 \cdots\cdots\cdots\cdots\cdots\cdots (6)$$

$$\ln(\beta) = d - e M_0 \cdots\cdots\cdots\cdots\cdots\cdots (7)$$

where a,b,d and e are constants that depend on the regional characteristics and M_0 is the magnitude of the mainshock.

Equations (3) through (7) are combined to obtain the following relationship for the number of aftershocks as function of the mainshock:

$$N_a(M) = \exp(a + bM_0 + (c-M)\beta) \cdots\cdots\cdots (8)$$

and

$$\beta = \exp(d - eM_0) \cdots\cdots\cdots\cdots\cdots\cdots (9)$$

These formulations will be used to simulate the number of aftershocks for each mainshock of magnitude M_0.

It is assumed that magnitudes of aftershocks do not exceed the magnitude of the mainshock. Substituting $M_{max} = M_0$ into equation (4) yields:

$$f_M(m) = \frac{\beta e^{-\beta m}}{e^{-\beta M_{min}} - e^{-\beta M_0}} \quad \cdots\cdots\cdots (10)$$

Therefore, equation (10) will be used to describe the magnitudes of mainshocks.

4.2 Methodology

The occurrence times and the magnitudes of mainshocks in a lifetime of a structure are simulated first. The magnitudes and the number of aftershocks that belong to the mainshock are generated next. This produces a single sequence of mainshocks with their corresponding aftershocks. The epicenters for the mainshock-aftershock sequence are simulated and the epicentral distances are calculated. For each event in the sequence the response spectra, peak ground accelerations, and the durations of ground motions at the site are calculated. The time histories of ground accelerations for the sequence are calculated using the duration independent envelope function. Damage spectra of the ground motions are calculated. The damage spectra of ground motions in a sequence of mainshock-aftershock are calculated considering cumulative damage related with both the response deformation and the dissipated hysteretic energy of the SDOF during the sequence. In this step, for purpose to estimate relatively the damage potential of ground motions, we neglect the possibility that structures damaged by large ground motions might change their dynamic characteristics or might be reinforced. Finally, steps described above are repeated to obtain the average and the deviation of the damage spectra.

It is very useful for the design purpose to obtain the required yield strength ratio of ground motions with the average (or average+ σ) damage spectrum during the mainshock-aftershock earthquake sequences so as to satisfy a safety level with the damage index=1.0. The strength demand spectrum with uniform damage in the lifetime of a structure is defined to be the spectrum of the required yield strength ratio obtained like this. The strength demand spectrum can rationally reflect the seismic activities around the site by considering mainshock-aftershock earthquake sequences in desired design period of a structure.

4.3 Application to Eureka, California

The proposed method is applied to estimation of damage potential of ground motions and the strength demand spectrum with uniform damage in the lifetime of a structure in Eureka and Rio Dell, California. The parameters for the probabilistic occurrence model of the mainshock-aftershock sequences are developed according to the earthquake data near Eureka.

4.3.1 Mainshock-aftershock sequence model

The mainshock-aftershock sequences are modeled based on earthquake data near Eureka provided by the United States Geological Survey (USGS). There were 1519 earthquakes that occurred from 1940 to 1992 with magnitudes greater than or equal to 3.0, within the area bounded by latitudes from 39.5°N to 42°N, and longitude from 125°W to 123°W.

The earthquake clustering method developed by Veneziano and Van Dyck[11] was applied to discriminate aftershocks from earthquake data. In this method, clusters that consist of a mainshock and aftershocks are statistically tested and discriminated with a specified significance level. The amount of discriminated aftershocks is 52% of all the earthquakes in the database.

Figure 3 shows sequences of mainshocks which occurred from 1940 to 1992 with magnitudes greater than 5.0. The interarrival time distribution for the mainshocks was determined to be well represented using an exponential distribution. The parameter of exponential distribution was found to be 0.84. From the same data, the value of the slope β for the mainshocks is found to be 1.4.

Among the 1519 earthquakes, there are 11 clusters which consist of a mainshock with magnitude greater than or equal to 5.0 and more than 10 aftershocks. Table 2 shows the magnitude of the mainshock, the number of aftershocks with magnitudes greater than or equal to 3.0, and the β-value for aftershocks.

Based on the data in Table 2, a relationship is developed between the number of aftershocks with magnitudes greater than or equal to 3.0, $N_a(3)$, and the magnitude of the mainshock, M_0. Therefore, we obtain

$$N_a(M) = \exp(-0.64+0.67M_0+(3-M)\beta) \cdots\cdots (11)$$

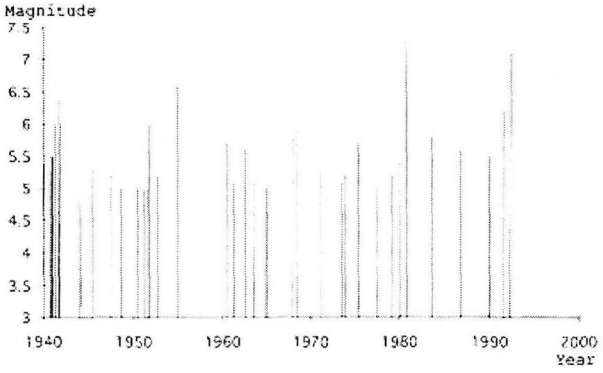

Figure 3 Sequence of mainshocks from 1940 to 1992 with magnitudes greater than or equal to 5.0

Table 2 Statistics of aftershock clusters

Cluster number	Magnitude of mainshock	Number of aftershocks	β-value
1	6.6	10	0.67
2	5.7	14	0.97
3	5.9	51	1.52
4	5.3	30	1.20
5	5.7	15	1.13
6	7.3	156	1.27
7	5.8	15	0.94
8	5.6	86	1.87
9	5.5	22	2.58
10	6.2	38	2.67
11	7.1	96	1.27

$$\beta = \exp(1.11\text{-}0.136M_0) \cdots\cdots\cdots\cdots\cdots\cdots (12)$$

Figure 4 shows the relationship between the number of aftershocks $N_a(M)$ and aftershock magnitude M as a function of the mainshock magnitude M_0 according to the equation (11).

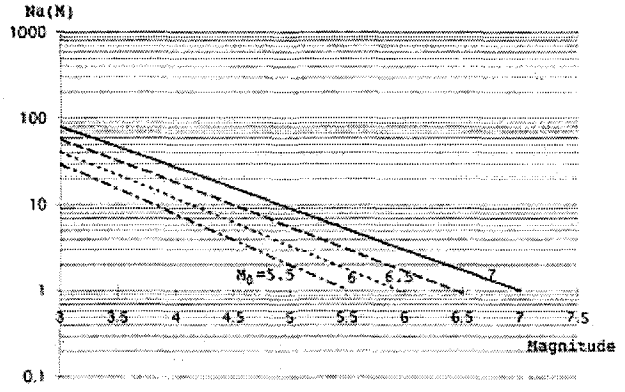

Figure 4 Relationship between the number of aftershocks $N_a(M)$ and aftershock magnitude M as a function of the mainshock magnitude M_0

4.3.2 Faults model

The generalized tectonic map of Northern California by Kelsey and Carver[12] was used to identify tectonic features in the region. The major faults are modeled as shown in Figure 5, and the geometric parameters are listed in Table 3, where the distance H is the perpendicular distance from the site to the fault, and L2, L1 represent the fault length as shown in the Figure 6.

In order to determine the distance from the rupture zone to the site of interest, it is assumed that the epicenters of the mainshocks occur with equal likelihood along the active faults, and the epicenters of the aftershocks are uniformly distributed along the rupture length of the mainshock. The rupture length of a mainshock can be related to its magnitude using the equations of Wells and Coppersmith[13] for strike-slip fault:

$$\log(L) = -2.57+0.624M \cdots\cdots\cdots\cdots\cdots\cdots (13)$$

where L is the rupture length and M is the moment magnitude of the mainshock.

4.3.3 Ground motion estimation method

Using the simulated magnitudes of mainshock-aftershock earthquake sequences and their epicenters, an appropriate ground motion attenuation function will give ground motions at the site. The attenuation equation developed by Boore et al.[14] is adopted for the purposes of the ground motion simulation. In this equation, the ground-motion parameter (peak horizontal acceleration or pseudo-acceleration response) is expressed by the magnitude of earthquake, the shortest distance from the site to the vertical projection of the earthquake fault rupture, and the average shear-wave velocity over 30 m in surface ground at the site.

A number of stochastic models have been proposed for generating the earthquake ground accelerations. Tung et al.[15]

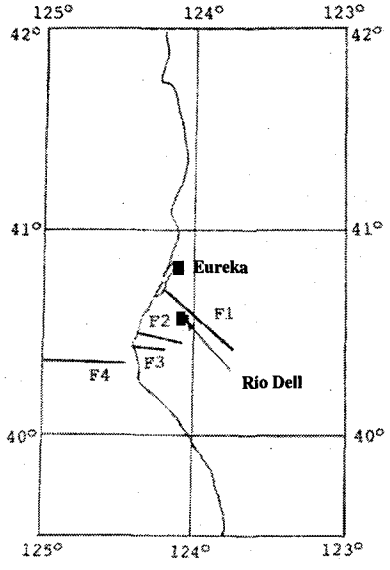

Figure 5 Map of fault model around Eureka and Rio Dell

Table 3 Geometric parameters of modeled faults for the site

Fault	Distance(km) H	Length(km) L1	Length(km) L2	
F1 (Little Salmon Fault)	10	-5	45	For Eureka
	5	-20	30	For Rio Dell
F2 (Russ Fault)	30	-12.5	12.5	For Eureka
	13	-2.5	22.5	For Rio Dell
F3	40	2.5	22.5	For Eureka
	18	5	25	For Rio Dell
F4 (Mendocino Fault Zone)	50	20	65	For Eureka
	25	30	75	For Rio Dell

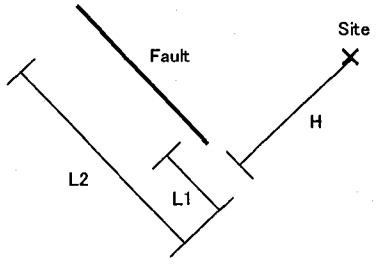

Figure 6 Geometric parameters of fault

used the ground motion simulation program SIMQKE with duration independent envelope function. This approach is adopted herein because it requires that very few parameters to be defined. The parameters needed include the response spectra, the duration of ground acceleration, and the peak ground acceleration.

The duration of ground acceleration depends on the duration of the rupture process, the magnitude of the earthquake, the epicentral distance and the soil conditions of the site. Usually larger earthquakes produce ground motions with longer durations. Although several other relations have been proposed for ground motion duration, the Bullen and Bolt[16] equation is used in the calculation of ground motion duration for its simplicity.

4.3.4 Results

The damage potential of ground motions considering mainshock-aftershock earthquake sequences at Eureka and Rio Dell, California is estimated by applying the simulation procedure described in **4.2.** The parameters for the probabilistic occurrence model of the mainshock-aftershock sequences described above are used.

Figure 7 shows damage potential of ground motions during mainshock-aftershock earthquake sequences in 50 years at Eureka and Rio Dell. In this figure, the upper two figures show damage spectra of ground motions by simulated 50 mainshock-aftershock earthquake sequences in 50 years, the bottom two figures show the average and the average plus/minus one standard deviation (σ). Figure 8 shows the damage potential of ground motions during only mainshocks in 50 years at Eureka and Rio Dell. Figure 9 shows comparison between average damage potential of ground motions in 50 years at Eureka and Rio Dell. Based on these figures, it is found that damage potential of ground motions at Rio Dell is significantly higher than damage potential at Eureka, and that the effect of aftershocks on damage potential of ground motion is statistically negligible in this area.

Figure 10 shows the strength demand spectra of ground motions with average damage potential in 50 years at Eureka and Rio Dell. The strength demand spectra of the ground motions are obtained so as to satisfy a safety level with the damage index=1.0. Figure 11 and Figure 12 show the strength demand spectra of ground motions with average and average+ σ damage spectrum in 50 years at Eureka and Rio Del, respectively. Based on these figures, it is found that the strength demand spectra at Rio Dell are significantly higher than those at Eureka. These strength demand spectra are very useful for design purpose. Based on the Figures 11 and 12, the required yield strength ratio of 0.35 and 0.5 can be taken for design of structures with natural periods smaller than 0.6 sec. at Eureka and Rio Dell, respectively.

5. Conclusions

The damage spectra of ground motions during large aftershocks of past earthquakes including the 1983 Coalinga earthquake and the 1987 Whittier Narrows earthquake in California were studied. Based on the examples, it can be concluded that the combination of mainshock-aftershock ground motions can be more damaging to structures than the ground motions from the mainshock alone.

A simulation methodology for damage spectra considering mainshock-aftershock earthquake sequences in the desired design period of a structure was presented. The simulation procedure consists of the following steps: (1) simulation of the occurrence times of mainshocks in a lifetime of a structure, (2) simulation of the magnitudes of the mainshocks, (3) calculation of the number of aftershocks which belong to each mainshock, (4) simulation of the magnitudes of aftershocks, (5) simulation of the epicenters for the mainshock-aftershock sequence, (6) calculation of the response spectra and the peak ground accelerations at the site for the sequence, (7) calculation of the duration times of ground accelerations, (8) calculation of the

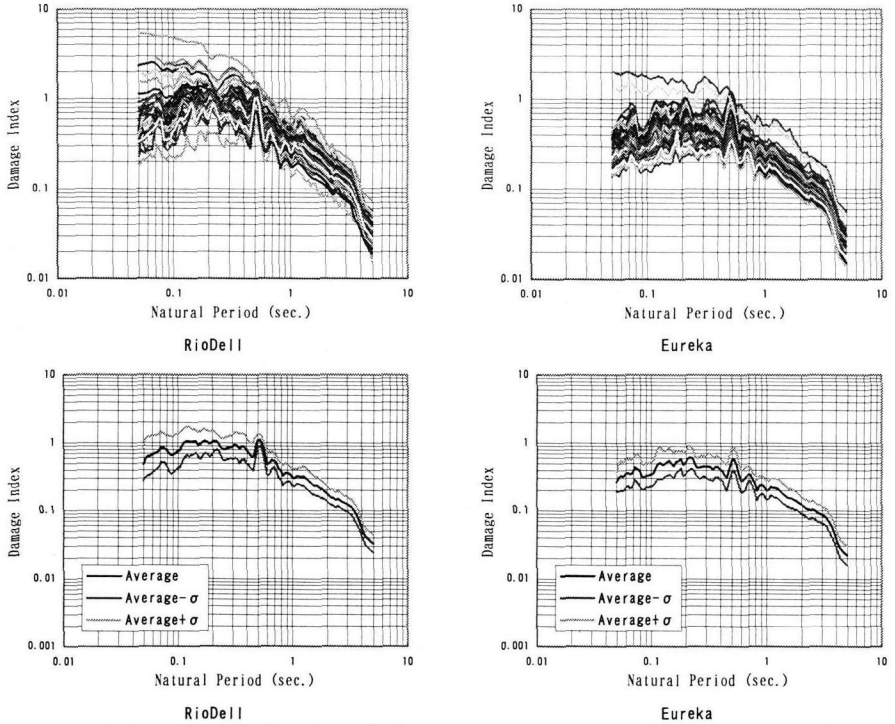

Figure 7 Damage potential of ground motions by mainshock-aftershock sequences in 50 years at Eureka and Rio Dell (The upper two figures show simulated 50 damage spectra, the bottom two figures show the ave. and the ave. plus/minus one standard deviation σ)

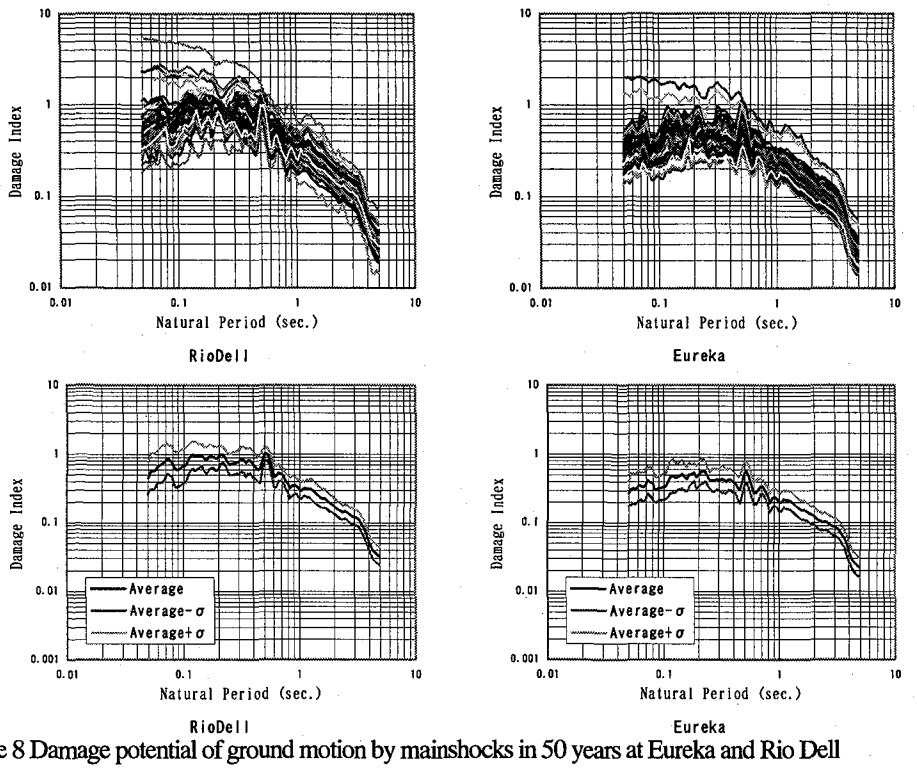

Figure 8 Damage potential of ground motion by mainshocks in 50 years at Eureka and Rio Dell
(The upper two figures show simulated 50 damage spectra, the bottom two figures show the ave. and the ave. plus/minus one standard deviation σ)

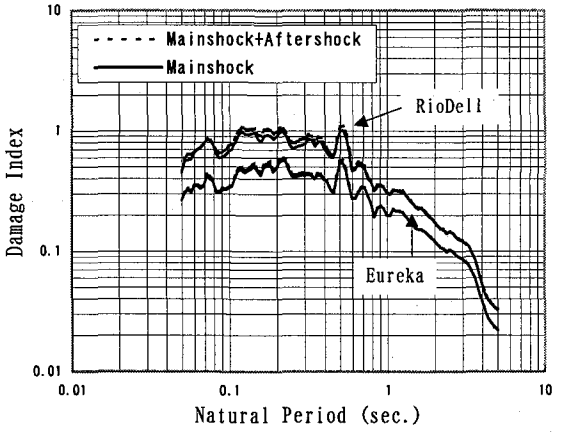

Figure 9 Comparison between average damage potential of ground motions in 50 years at Eureka and Rio Dell

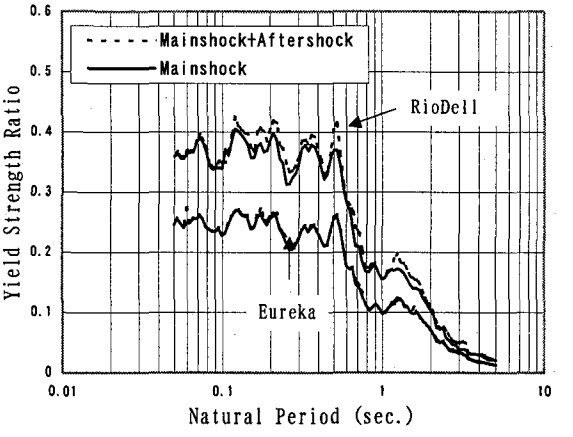

Figure 10 Strength demand spectra of ground motions with average damage potential in 50 years at Eureka and Rio Dell

time histories of ground accelerations, (9) calculation of the damage spectra of the ground motions for the sequence. Finally, steps (1) to (9) are repeated to obtain the average and the deviation of the damage spectra.

The strength demand spectrum with uniform damage level in the lifetime of a structure is defined to be the spectrum of the required yield strength ratio of ground motions with the average (or average + σ) damage spectrum during the mainshock-aftershock earthquake sequences so as to satisfy a safety level with the damage index=1.0. The strength demand spectrum is very useful for the design and can rationally reflect the seismic activities around the site by considering mainshock-aftershock earthquake sequences in desired design period of a structure.

The proposed method was applied to estimation of damage potential of ground motions considering mainshock-aftershock earthquake sequences in Eureka and Rio Dell, California. The parameters for the probabilistic occurrence model of the mainshock-aftershock sequences were modeled based on earthquake data near Eureka provided by the United States Geological Survey (USGS). Based on the results, it is found that the strength demand spectra at Rio Dell are significantly higher than those at Eureka. The required yield strength ratio of 0.35 and 0.5 can be taken for design of structures with natural periods smaller than 0.6 sec. at Eureka and Rio Dell, respectively. The strength demand spectra obtained like this can rationally reflect

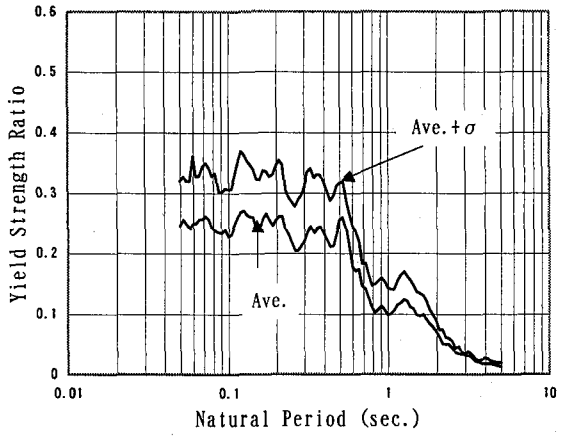

Figure 11 Strength demand spectra of ground motions with average and average+ σ damage potential in 50 years at Eureka

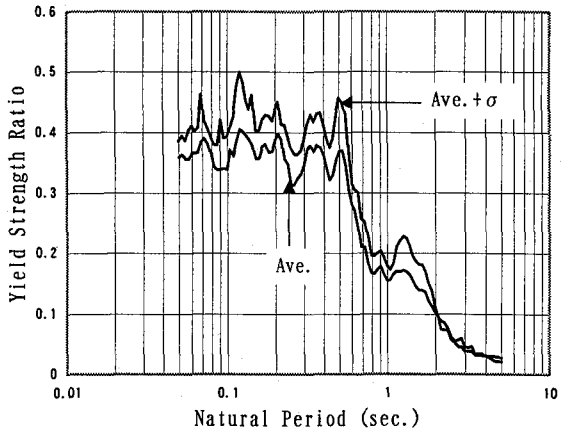

Figure 12 Strength demand spectra of ground motions with average and average+ σ damage potential in 50 years at Rio Dell

the seismic activities around the site by considering mainshock-aftershock earthquake sequences in desired design period of a structure.

References

1) Priestley, M. J. N., The Whittier Narrows, California earthquake of October 1, 1987 - damage to the I-5/I-605 separator, *Earthq. Spectra*, Vol.4, No.2, 389-405, 1988.
2) EQE Engineering, The July 16, 1990 Philippines earthquake, a quick look report, 1990.
3) Sunasaka, Y., Damage spectra of ground accelerations during earthquakes, Proc. ICOSSAR, Vol.3, 1699-1702, 1998.
4) Sunasaka, Y., T. Toki and A. S. Kiremidjian, Evaluation of damage potential of ground motion during great earthquakes, *Earthquake Spectra* (on application).
5) Park, Y. J. and A. H.-S. Ang, Mechanistic seismic damage model for reinforced concrete, *Jour. Struct. Eng., ASCE*, Vol.111, No.4, 740-754, 1985.
6) Park, Y. J. and Ang A. H.-S., Wen Y. K., Seismic damage analysis of reinforced concrete buildings, *Jour. Struct. Constr. Eng., ASCE*, Vol.111, No.4, 722-739, 1985.
7) Sunasaka, Y. and A. S. Kiremidjian, A method for cumulative damage estimation from mainshock-aftershock earthquake sequences, Proc. of the Fifth U.S. National Conference on Earthquake Engineering, Vol. I, 481-490, 1994.
8) Anagnos, T. and A. S. Kiremidjian, Stochastic time -predictable model for earthquake occurrences, *Bull. Seism. Soc. Am.*, Vol.74, 2593-2611, 1984.
9) Kiremidjian, A. S. and T. Anagnos, Stochastic slip predictable model for earthquake occurrences, *Bull. Seism. Soc. Am.*, Vol.74, 739-755, 1984.
10) Utsu, T., A statistical study on the occurrence of aftershocks, *Geophys. Magazine*, Vol.30, No.1, 521-616, 1961.
11) Veneziano, D. and J. Van Dyke, Statistical discrimination of aftershocks and their contribution to seismic hazard, *Consulting Report to Dames & Moore, Golden*, Colorado, 1984.Kelsey, H. M. and G. A. Carver, Late neogene and quaternary tectonics associated with northward growth of the San Andreas transform fault, northern California, *Jour. Geophys. Res.*, Vol.93, No.B5, 4797-4819, 1988.
12) Kelsey, H. M. and G. A. Carver, Late neogene and quaternary tectonics associated with northward growth of the San Andreas transform fault, northern California, *Jour. Geophys. Res.*, Vol.93, No.B5, 4797-4819, 1988.
13) Wells D. L. and K. J. Coppersmith, New empirical relationships among magnitude, rupture length, rapture width, rapture area and surface displacement, *Bull. Seism. Soc. Am.*, Vol.84, No.4, 947-1002, 1994.
14) Boore, D. M., W. B. Joyner and T. E. Fumal, Equations for estimating horizontal response spectra and peak acceleration from Western North American earthquakes: A summary of recent work, *Seismological research Letters*, Vol.68, No.1, January/February, 128-151, 1997.
15) Tung, A. T. Y., J. N. Wang, A. S. Kiremidjian and E. Kavazanjian, Statistical parameters of AM and PSD functions for generation of site-specific strong ground motions, *Proc. Tenth World Conference Earthq. Eng.*, Madrid, Spain, 867-872, 1992.
16) Bullen, K. E. and A. B. Bolt, *An introduction to the theory of seismology*, Cambridge University Press, 1985.

(Received September 14,2001)